

Selective excitation of surface-polariton Bloch waves for efficient transmission of light through a subwavelength hole array in a thin metal film

Yong Zeng,^{1,2} Y. Fu,¹ Xiaoshuang Chen,² Wei Lu,² and H. Ågren¹

¹*Department of Theoretical Chemistry, School of Biotechnology, Royal Institute of Technology, AlbaNova, S-106 91 Stockholm, Sweden*

²*National Laboratory for Infrared Physics, Shanghai Institute of Technical Physics, Chinese Academy of Science, 200083 Shanghai, China*

(Received 11 January 2007; revised manuscript received 7 March 2007; published 23 July 2007)

Electromagnetic (EM) field was found to be able to transmit efficiently through a subwavelength hole array in a metal thin film at specific resonant frequencies. By analyzing the near-field distributions of EM fields in the array system, as well as the corresponding Fourier spectra, we show that the surface-polariton (SP) Bloch waves focus the energy of the incident plane-wave EM field to the vicinity of the hole at resonances (through SP scattering provided by the periodic hole). Furthermore, the wave vectors of the SP waves that contribute to the focusing effect are quantized as functions of the geometric shape of the holes in such a way that the focusing effect of the EM energy into the hole is maximal. The transmission efficiency and bandwidth at resonances are found to partially depend on the number of SP modes which contribute to the focusing effect.

DOI: 10.1103/PhysRevB.76.035427

PACS number(s): 78.20.Bh

In 1998, Ebbesen *et al.* reported light transmission through subwavelength hole arrays inside a silver film which was much higher than the hole-surface-to-total-surface ratio, even up to 2–3 orders of magnitude larger than that predicted by the conventional aperture theory.^{1,2} The results have received much experimental^{3–5} and theoretical attention.^{6–12} In attempts to understand the underlying physical mechanisms, many aspects of the structure have been studied, including the arrangement of the subwavelength holes,¹ the thickness of the metal film,³ the polarization of the incident light,⁴ the hole shape,⁴ and the symmetry of the whole structure.¹³ Many explanations about the experiments of Ebbesen *et al.* have been presented, such as the appearance of localized waveguide resonances⁶ and the dependence of the resonances on the hole geometric shape (shape resonance).⁴ In addition, various complicated hole array structures have been proposed for even better light transmission efficiency.^{14,15}

The surface-polariton (SP) Bloch waves are known to exist in the spatial periodic hole array in a metal film. With the normal incidence of an external excitation light, the wave vector of an excited SP Bloch wave can be written as⁷

$$\mathbf{K}_{sp} = p \frac{2\pi}{L} \mathbf{u}_x + q \frac{2\pi}{L} \mathbf{u}_y, \quad (1)$$

where \mathbf{u}_x and \mathbf{u}_y are the unit reciprocal lattice vectors of the periodic hole array, L is its period, and p and q are integer numbers determining the SP propagation direction. Moreover, the low-order [i.e., $(p, q) = (\pm 1, 0)$ or $(0, \pm 1)$] SP Bloch waves have been shown to play very important roles in the extraordinary optical transmission.^{3,12} Notice that the wave vector of the excited SP Bloch waves is totally determined by the period of the hole array, as shown in Eq. (1). On the other hand, experimental and theoretical studies have demonstrated that the transmission spectrum of the hole array depends on the geometric shape of the holes.^{4,6} In this work, we concentrate on the physical mechanism of such a dependence by calculating the near-field electromagnetic (EM) field distribution. We will also show that the high-order

($|\mathbf{K}_{sp}| \geq 4\pi/L$) SP Bloch waves effectively focus the EM field to the vicinity of the hole, resulting in directly the observed extraordinary light transmission.

We consider a freestanding silver film perforated by an array of holes, see Fig. 1. The thickness of the metal film is denoted as h , the hole has a square cross section of $a \times a$, and the square hole array has a period of L in the xy plane. Due to the symmetry along the z direction, double-resonance phenomenon will appear in this structure; i.e., identical SP Bloch waves will be excited on the two metal-air surfaces of the metal film.¹³ The relative dielectric constant of silver is given by the Drude model of

$$\epsilon(\omega) = 1.0 - \frac{\omega_p^2}{\omega(\omega + i\gamma)}, \quad (2)$$

where $\omega_p = 1.374 \times 10^{16} \text{ s}^{-1}$ is the bulk plasma frequency and $\gamma = 3.21 \times 10^{13} \text{ s}^{-1}$ is the damping rate. These values are obtained by fitting the experimental results in the wavelength region [750,900] nm.¹⁶

The numerical calculation approach for the EM field is based on the Fourier modal method,^{17–20} which has been used to calculate the transmission spectrum of one-

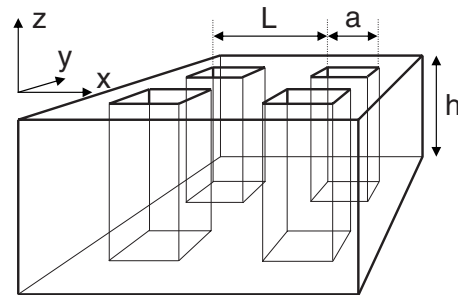


FIG. 1. Schematic drawing of a freestanding silver film perforated with a square array of square air holes. h is the thickness of the metal film, the hole has a square cross section of $a \times a$, and the square array has a period of L .

dimensional and two-dimensional metal gratings.^{4,11} The fundamental physical background of this method involves the (1) expression of the EM field in the surrounding homogeneous medium by Bragg waves. For the normal incident plane wave propagating along the z axis with a wave vector $\mathbf{k}_0=(0,0,k_{0z})$, the EM field can be expressed as a superposition of Bragg waves:

$$\mathbf{E}(\mathbf{r}) = \sum_{ij} \mathbf{E}_{ij}(z) e^{i(k_{ij,x}x + k_{ij,y}y)}, \quad (3)$$

$$\mathbf{H}(\mathbf{r}) = \sum_{ij} \mathbf{H}_{ij}(z) e^{i(k_{ij,x}x + k_{ij,y}y)}, \quad (4)$$

where the wave vector $\mathbf{k}_{ij}=2\pi(i\mathbf{u}_x + j\mathbf{u}_y)/L$. It also involves the (2) expression of the EM field in the metal grating (the hole array in our case) by the corresponding eigenmodes, (3) use of the boundary conditions among EM fields in the metal grating and two neighboring homogeneous medium to obtain the transfer matrix or scattering matrix, and (4) use of the obtained transfer matrix to calculate the transmission spectrum of the whole structure as well as the EM field distribution. In principle, the method is only limited by the finite number of Bragg waves which can be included in numerical calculations. The problem is normally solved by the convergence of the numerical results as functions of the number of Bragg waves. In our case, 21×21 plane waves have been applied, and the numerical values have been cross-checked by comparing the numerical results with ones from 31×31 plane waves. In addition, one must pay special attention to the way of expressing the products of Fourier series involved in the eigenmode problem (the details can be found in Ref. 17).

We first study the effect of the thickness h of the metal film on the optical properties of the subwavelength hole array. The array period L and hole side length a are fixed to be 750 and 280 nm, respectively, while h increases from 100 to 800 nm, which were studied earlier.^{3,11} The transmission spectrum is calculated for a circularly polarized plane wave at normal incidence to the metal film, and the results are plotted in Fig. 2. Transmission peaks have been obtained, which are known to be the results of the resonances of SP Bloch waves.³ The resonance peaks depend strongly on the metal film thickness h . More than two resonances are observed when h changes between 100 and 400 nm, while there is only one resonance at 802 nm when h is thicker than 500 nm. The underlying mechanism is similar to that of an EM plane wave incident on a thin continuous metal film (not perforated by holes). When the metal film is thin enough, the SP on one of the two metal-air surfaces will interact strongly with the other one which is localized on the other metal-air surface so that a ‘‘repulsion of the levels’’ occurs.²¹ A direct evidence of such a repulsion is that the sum of the SP mode energies (given as $2\pi c\hbar/\lambda = \hbar\omega$) of these two resonances [for the same h in Figs. 2(b) and 2(d)] is close to twice the energy at 802 nm [Fig. 2(e)] when the film is thick enough (thus the two SPs at the two surfaces are not correlated). This phenomenon can also be explained by the modification of the dispersion relation of the two-dimensional hole array,⁶ that is, a weak interaction between two air/metal surfaces modi-

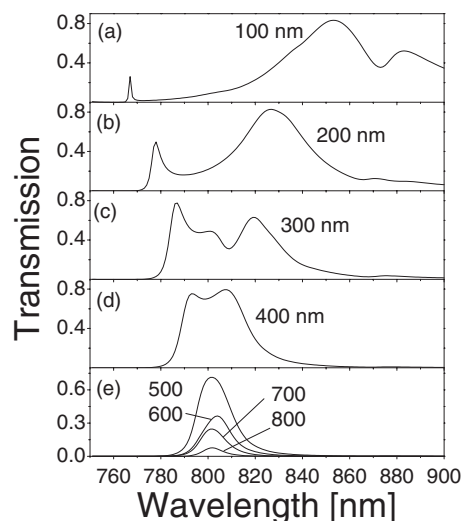


FIG. 2. Normal incident transmission spectra of a silver film perforated with a square array of square hole. $L=750$ nm and $a=280$ nm. The metal film thickness h increases from 100 to 800 nm.

fies the original band structure of the periodic hole array. The second interesting phenomenon is that the transmission magnitudes and bandwidths of the two resonances are significantly different. The low-energy transmission resonance always has a high magnitude and a wide bandwidth. These are the direct effects of the SP Bloch waves.

To elucidate the roles of SP Bloch waves in the transmission resonances and their relationships with the transmission magnitudes and bandwidths, we have calculated and plotted the near-field distributions of the transmitted light on a surface at a distance of 1 nm above the metal-air surface at three resonant wavelengths, see Figs. 3(a1)–3(c1). As a comparison, the near-field distributions of the reflected light on a surface at a distance of 1 nm from the other metal-air surface at the same resonant wavelengths have also been plotted [Figs. 3(a2)–3(c2)]. Clearly, the field distribution of the transmitted light is very similar to the reflected light. In the following, we denote the 802 nm resonance of $h=700$ nm as the first resonance [Figs. 3(a1) and 3(a2)], the 767 nm resonance of $h=100$ nm as the second resonance [Figs. 3(b1) and 3(b2)], and the 853 nm resonance of $h=100$ nm as the third resonance [Figs. 3(c1) and 3(c2)]. Only an x -polarized normal incident plane wave is considered because of the symmetry in the xy plane of our structure. Three important properties of these near-field distributions can be observed.

First, the EM field at resonance is strongly localized in the vicinity of the hole. We use a ratio η between the average intensities ($|E_x^2|$) inside and outside the hole (in the xy plane)

$$\eta = \frac{A_{\text{cell}} - A_{\text{hole}}}{A_{\text{hole}}} \frac{\int_{\text{inside}} |E_x^2| dx dy}{\int_{\text{outside}} |E_x^2| dx dy} \quad (5)$$

to describe the degree of such a localization, where $A_{\text{hole}}=a^2$ is the area of the hole and $A_{\text{cell}}=L^2$ is the area of a unit

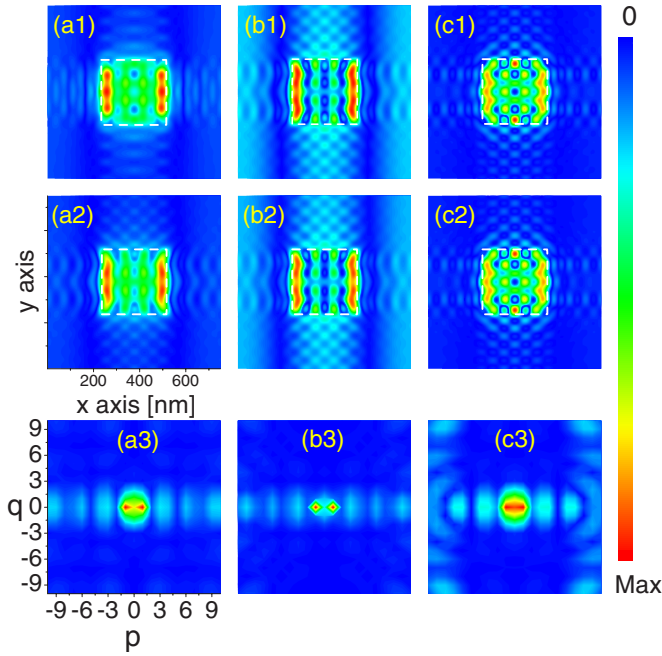


FIG. 3. (Color online) Intensity ($|E_x^2|$) distributions of the transmitted and reflected light across a unit cell of the periodic array at wavelengths of [(a1) and (a2)] 802 nm (resonance when $h = 700$ nm), [(b1) and (b2)] 767 nm (high-energy resonance when $h = 100$ nm), and [(c1) and (c2)] 853 nm (low-energy resonance when $h = 100$ nm) at a distance of 1 nm from the metal-air surface. The incident light is polarized along the x direction (because the x direction is identical to the y direction in our structure). The corresponding Fourier spectra $f(p, q)$ are also plotted in (a3), (b3) and (c3) for these three resonance wavelengths. White dashed lines mark the position of the hole.

cell in the periodic structure. Note that the ratio between the average intensity inside the hole and that of the unit cell is $\eta/[1-(1-\eta)s]$, where $s=A_{\text{hole}}/A_{\text{cell}}$. It should also be emphasized here that for two special structures, without metal film ($A_{\text{hole}}=A_{\text{cell}}$) and without air hole ($A_{\text{hole}}=0$), the η defined in the above equation is to be replaced by $\lim_{A_{\text{hole}} \rightarrow A_{\text{cell}}} \eta$ and $\lim_{A_{\text{hole}} \rightarrow 0} \eta$, and both equal to unity. η varies significantly for different resonances, it is 8.5 for the first resonance, 29.5 for the second resonance, and 61.2 for the third one. Whereas the hole-surface-to-unit-cell-surface ratio is only 0.14, it is very surprising to notice that as high as 91% of the intensity becomes localized inside the hole at the third resonance. In other words, the majority of the light becomes “focused” inside the hole. It should be pointed out that there exists a direct relationship between the ratio η and the transmission coefficient; that is, a strong localization leads to a high transmission coefficient. We can, in general, decompose the light transmission process into two principal steps; the EM field is first focused into the hole area on the metal-air surface, and then it propagates through the hole. Our numerical calculations indicate that the lowest propagating decay ratio is almost identical for all metal films of different thicknesses and frequencies of the incident light under investigation, which is probably due to the fact that no waveguide modes are allowed in these films.⁹ It can thus be concluded that such a field localization process (the EM field becomes

focused into the hole area on the metal-air surface) is directly responsible for the observed extraordinary light transmission.

Second, fine structures, in the form of regular ripples, of SP Bloch waves are observed in the EM intensity distributions, where the spatial interval is about $L/12$ between two neighboring lobes in Fig. 3(a2). Meanwhile, for Figs. 3(b1) and 3(b2) (the second resonance), a clear interference of two SP Bloch waves of $(p, q) = (\pm 1, 0)$ exists along the x direction, which results in a relatively high electric field in the corresponding region. On the contrary, Figs. 3(c1) and 3(c2) show that, at the third resonance, the pattern of the field distribution on the metal-air surface is almost circular and the majority of the light becomes focused into the hole. Because the interval of the bright lobes inside the hole is much smaller than that of the other two resonances, many high-order SP Bloch waves contribute collectively to this resonance. The appearance of these high-order SP Bloch waves can be viewed as a picture of the repulsion of the levels discussed above. Similar result has also been obtained from our time-domain analysis: when a femtosecond light pulse is incident on this metal film, the third resonance is found to become excited only within the first tens of femtoseconds, while the second resonance dominates the forthcoming 300 fs. Since higher-order SP Bloch waves decay very fast, it is then reasonable to deduce that they contribute collectively within the first tens of femtoseconds to the third resonance.²² On the other hand, the air holes can be viewed as surface defects on an originally perfect metal film, which will scatter the SP waves from high-order Bloch modes to low-order modes, even light,²¹ so that a large number of participating high-order SP Bloch waves indicate an increased possibility for the localized SP wave to be scattered into propagating light. It is the collective propagations and interactions of these SP Bloch waves that effectively focus the EM field into the hole. In order to obtain a strong “focusing” effect, the SP Bloch waves, at the transmission resonances should destructively interact among themselves outside the hole region, whereas constructive interactions are expected inside the hole.

Third, a high degree of symmetry is present in every intensity distribution, reflecting the boundaries of the Brillouin zone of the periodic hole array.⁷ Referring to the 802 nm resonance (the first resonance), there are a total of 16 bright lobes which are evenly arranged inside the hole with a spatial interval of $\Delta = 72$ nm in both the x and y directions, which is expected to be a quarter of the spatial boundary a' of the electric field (where the electric field is close to zero). The spatial boundary of the electric field is largely determined by the hole size a (280 nm); it is, however, larger than a after taking into account the skin effect. This explains why Δ ($=72$ nm) in our case is slightly larger than $a/4$ ($=70$ nm). Based on such a relationship between the interval of bright lobes Δ and the hole size a , it is concluded that the hole geometric shape affects the EM field distribution inside the hole significantly.

In order to compare the contributions of different SP Bloch waves to these resonances, we perform a Fourier transform on the electric field distributions

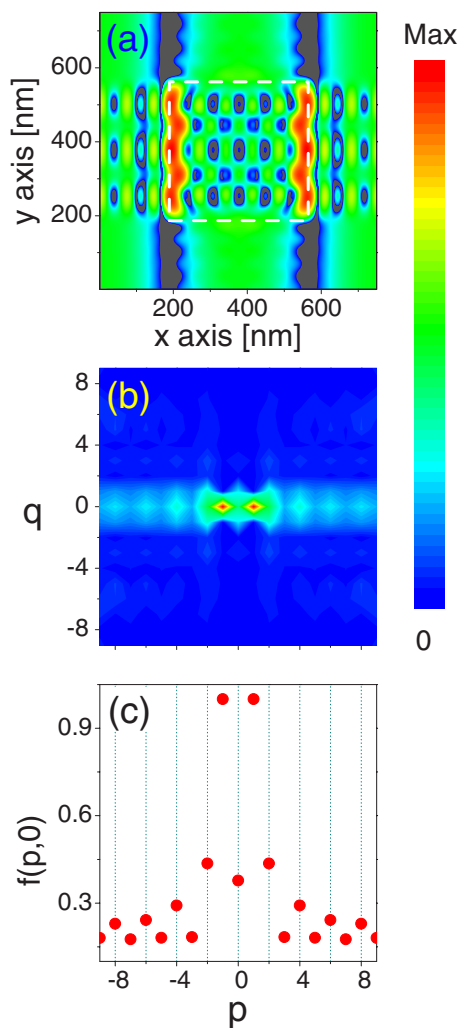


FIG. 4. (a) (Color online) Intensity ($|E_x^2|$) distributions of the transmitted light across a unit cell at a resonant wavelength of 763 nm, at a distance of 1 nm from the metal-air surface. (b) The corresponding Fourier spectrum $f(p, q)$. (c) The Fourier spectrum $f(p, q=0)$. The structure considered here is a freestanding silver film perforated with a square array of square air holes, and relevant parameters are $L=750$ nm, $a=375$ nm, and $h=100$ nm. Polarization of the incident light is along the x direction (because the x direction is identical to the y direction in our structure). White dashed lines mark the position of the hole.

$$f(p, q) = \left| \frac{1}{f(1,0)} \int_{\text{cell}} E_x(x, y) e^{ip(2\pi/L)x} e^{iq(2\pi/L)y} dx dy \right|, \quad (6)$$

where $E_x(x, y)$ is the electric field, p and q are integers, and $f(p, q)$ is normalized with respect to $f(1, 0)$. Results are plotted in Figs. 3(c1)–3(c3). Notice that the data are actually discrete, even the images look continuous [see more details in Fig. 4(c)]. It should emphasize that, because of the periodicity of $E_x(x, y)$ in the whole xy plane, the wave vector used here [$(p, q)2\pi/L$] implies that we Fourier transform the electric field in the whole xy plane, but not just one unit cell.

Therefore, the finite integral region absolutely has no effect on the profile of the Fourier spectrum.

An interesting “quantization effect” is observed in these figures: The peak positions of $f(p, q)$ [not $f(p, q)$ itself] are not continuous functions of p and q ; they are discrete [see Fig. 4(c) as an example]. At the wavelength of 802 nm [Fig. 3(c1)], $f(\pm 1, 0)$ is maximal (which is most probably related to the localized electronic oscillations close to the edge of the hole⁷), $f(\pm 2, 0)$ is almost zero, and $f(\pm 3, 0)$ is $0.24f(\pm 1, 0)$. This looks very surprising since a high-order SP Bloch wave is normally expected to decay much faster than a low-order SP Bloch wave along the z direction (given by $e^{-k_z z}$) because of $k_z = i\sqrt{k_x^2 + k_y^2 - k_0^2}$. Here, k_0 is the wave vector of the incident wave in vacuum. On the other hand, the influence of high-order SP Bloch waves has already been observed in the near-field distributions. The in-plane momentum of the high-order SP Bloch waves corresponding to the $f(p, q)$ peak can be expressed approximately as nk_{\min} , where n is an integer, $k_{\min} = \alpha(2\pi/L)$. $2\pi/L$ is the minimal Bloch wave vector in our periodic system. $\alpha \approx 3$ is obtained from the Fourier transform results of Figs. 3(a3)–3(c3). On the other hand, we also notice that $k_{\min} \approx 2\pi/a$ (because the air hole can be viewed as a metal waveguide), so that α is expected to equal approximately the ratio between the period L of the hole array and the hole size a , which is 2.68 for the structure of Fig. 3. This is not a mere coincidence. It has already been reflected in the interference of these discrete SP Bloch waves, which results in the high degree of symmetry in the intensity distribution. The difference between 3 and 2.68 in the above relationships is most probably induced by the collective interactions among the SP waves generated on the two metal-air surfaces. Another array structure with $L/a=2$ has been studied for further elucidation, and the intensity distribution as well as the corresponding Fourier spectrum at one resonance are plotted in Fig. 4. Clearly, in this case, k_{\min} equals exactly $2(2\pi/L) = 2\pi/a$, as shown in Fig. 4(c). Therefore, the geometric shape of the holes in the array not only affects the form of waveguiding modes in the light transmission through the holes, as was concluded in Refs. 4 and 6, it also principally determines the excitation of SP Bloch waves in the energy focusing process. The lattice structure of the hole array also significantly affects the excitation of SP Bloch waves, as clearly indicated by their wave vector [Eq. (1)].

In Fig. 3, the nonzero $f(p, q)$ is largely condensed along the axis of $q=0$, which is due to the x polarization of the incident EM wave. The in-plane wave vector of a SP Bloch wave satisfies the following relationship¹¹:

$$k_{\text{SP}} \cdot H_y = 0, \quad (7)$$

so that the polarization of the incident plane wave determines the symmetry of the SP Bloch waves that participate in the resonance transmission.

It must be emphasized here that the light transmission coefficient of subwavelength hole arrays is totally determined by $f(0, 0)$ of the transmission light since only this zero-order mode, i.e., $(p, q)=(0, 0)$, is the exclusive propagating mode. $f(0, 0)$ equals 0.73 for the first resonance, 0.26

for the second resonance, and 0.93 for the third resonance. These values are much bigger than the hole-surface-to-unit-cell-surface ratio of 0.14, which corresponds to the $f(0,0)$ value when there is no SP wave generation. The underlying mechanism of such an enhanced $f(0,0)$ value is the scattering of SP waves by holes. In other words, the localized EM waves (SP waves) undergo radiative damping processes and become delocalized.⁷

The number of participating SP Bloch waves for the three resonances is very different, having the smallest value for 767 nm and the largest for 853 nm. This partially explains the difference in the corresponding transmission coefficient, see Fig. 2. A large number of SP Bloch waves [equivalently, a large number of the high-order SP waves; see Fig. 3(c3)] means that a large amount of the EM energy is transferred from the outside to the inside of the hole, leading to the observed strong light transmission via radiative damping processes. In addition, the high-order SP Bloch waves decay quickly along the z direction because of the large amplitude of the imaginary wave vector in this direction, so that the corresponding photon lifetime is small, which leads to the wide bandwidth when the number of the participating SP waves is large.³

Reference 23 discussed the difference between a perfect-electric-conductor-model (PEC) metal with a real metal (e.g., the Drude-model metal used here). In our structure, the maximal transmission is obtained for a thin metal film at a resonance frequency due to the repulsion of the levels and the radiation damping of SP waves scattered by holes contributes to the transfer of EM energy from a localized SP mode to a propagating zero-order mode. However, no real SP waves are allowed on a PEC metal-dielectric surface,⁸ so that no repulsion of the levels occurs (which means that the resonant frequencies do not depend on the thickness of the PEC

film). In this case, the process of light transmission through the holes in a PEC metal becomes the dominant factor in the whole transmission process.

In summary, we have studied the enhanced EM field transmissions through subwavelength hole arrays in metal-thin films, with different hole sizes and metal-film thicknesses, by analyzing the near-field distribution at the specific resonant frequencies, as well as the corresponding Fourier spectra. Due to the scattering by the holes, high-order SP Bloch waves are found to focus the EM energy into the hole area, leading to the enhanced resonance transmission. The magnitude and bandwidth of the resonance transmission are determined partially by the number of the SP waves that contribute to the focusing effect. Furthermore, an interesting quantization effect has been observed in the Fourier spectrum of the field distribution: The wave vectors of the SP waves that contribute to the focusing effect are quantized as functions of the geometric shape of the holes. Every detail of the subwavelength hole array structure including the hole geometrical size, the period of the hole array, the polarization of the incident EM wave, the material properties, and thickness of the metal film determines the SP waves collectively and selectively to maximize the localization of the EM energy inside the hole, i.e., the energy focusing process.

We thank Mats Bengtsson of the Royal Institute of Technology for invaluable help in Fourier transforming the field distributions. This work is partially supported by the Swedish Strategic Research Council (SSF) through a grant for research collaboration with Zhejiang University, China, within biophotonics. Computing resources from the Swedish National Infrastructure for Computing are acknowledged. This work is also partially supported by the Chinese Scholarship Council and the One-Hundred-Person Project of the Chinese Academy of Sciences (Grant No. 200012).

-
- ¹T. W. Ebbesen, H. J. Lezec, H. F. Ghaemi, T. Thio, and P. A. Wolff, *Nature (London)* **391**, 667 (1998).
- ²H. A. Bethe, *Phys. Rev.* **66**, 163 (1944).
- ³L. Martin-Moreno, F. J. Garcia-Vidal, H. J. Lezec, K. M. Pellerin, T. Thio, J. B. Pendry, and T. W. Ebbesen, *Phys. Rev. Lett.* **86**, 1114 (2001).
- ⁴K. L. van der Molen, K. J. K. Koerkamp, S. Enoch, F. B. Segerink, N. F. van Hulst, and L. Kuipers, *Phys. Rev. B* **72**, 045421 (2005).
- ⁵W. L. Barnes, W. A. Murray, J. Dintinger, E. Devaux, and T. W. Ebbesen, *Phys. Rev. Lett.* **92**, 107401 (2004).
- ⁶Z. Ruan and M. Qiu, *Phys. Rev. Lett.* **96**, 233901 (2006).
- ⁷L. Salomon, F. Grillot, A. V. Zayats, and F. de Fornel, *Phys. Rev. Lett.* **86**, 1110 (2001).
- ⁸J. B. Pendry, L. Martin-Moreno, and F. J. Garcia-Vidal, *Science* **305**, 847 (2004).
- ⁹K. J. Webb and J. Li, *Phys. Rev. B* **73**, 033401 (2006).
- ¹⁰H. F. Ghaemi, T. Thio, D. E. Grupp, T. W. Ebbesen, and H. J. Lezec, *Phys. Rev. B* **58**, 6779 (1998).
- ¹¹P. Lalanne, C. Sauvan, J. P. Hugonin, J. C. Rodier, and P. Chavel, *Phys. Rev. B* **68**, 125404 (2003).
- ¹²E. Popov, M. Neviere, S. Enoch, and R. Reinisch, *Phys. Rev. B* **62**, 16100 (2000).
- ¹³S. A. Darmanyan and A. V. Zayats, *Phys. Rev. B* **67**, 035424 (2003).
- ¹⁴F. I. Baida and D. Van Labeke, *Phys. Rev. B* **67**, 155314 (2003).
- ¹⁵F. J. Garcia de Abajo, G. Gomez-Santos, L. A. Blanco, A. G. Borisov, and S. V. Shabanov, *Phys. Rev. Lett.* **95**, 067403 (2005).
- ¹⁶*Handbook of Optical Constants of Solids*, edited by E. D. Palik (Academic, Orlando, 1985).
- ¹⁷L. Li, *J. Opt. Soc. Am. A* **14**, 2758 (1997).
- ¹⁸Y. Zeng, Y. Fu, X. Chen, W. Lu, and H. Ågren, *Phys. Rev. E* **73**, 066625 (2006).
- ¹⁹Y. Zeng, Y. Fu, X. Chen, W. Lu, and H. Ågren, *Solid State Commun.* **139**, 328 (2006).
- ²⁰Z. Y. Li and L. L. Lin, *Phys. Rev. E* **67**, 046607 (2003).
- ²¹A. V. Zayats, I. I. Smolyaninov, and A. A. Maradudin, *Phys. Rep.* **408**, 131 (2005).
- ²²Y. Zeng, Y. Fu, X. Chen, W. Lu, and H. Ågren (unpublished).
- ²³H. Shin, P. B. Catrysse, and S. Fan, *Phys. Rev. B* **72**, 085436 (2005).